2024 IEEE 63rd Conference on Decision and Control (CDC)
December 16-19, 2024. MiCo, Milan, Italy

Extended Object Tracking Under a State-Coupled Model with Gaussian Mixture Distribution

Zhifei Li[1], Chunsheng Liu[2], Shuli Ma[1] and Hongyan Wang[1]

Abstract— **This work proposes a state-coupled model (SCM) for extended object tracking, which treats the orientation and velocity as two dependent variables. With this model, the distribution of multiple measurements is modeled via Gaussian mixture density to match the actual automotive radar or Lidar data. As a result, SCM becomes a highly nonlinear model with multiplicative noise. To handle this challenge, we use the deterministic sampling approach to update the kinematics and orientation information, followed by a constraint condition. And the extent parameters are estimated under a Bayesian framework with pseudo-measurements. An evaluation is conducted on simulated data, which illustrates that the proposed model and filter are effective.**

I. INTRODUCTION

In recent years, the increased resolution capabilities of modern sensors (e.g., millimeter wave radar) have garnered attention in many scenarios, such as autonomous driving, region surveillance, and object tracking [1]. In this case, a sensor will receive multiple point-cloud measurements per object. Therefore, it becomes necessary to incorporate the object's spatial extent into the kinematics estimation process. This induces a so-called extended object tracking (EOT) problem. For this purpose, a variety of relevant models are given, including the random matrix (RM) for ellipse [2], [3], multiplicative error model (MEM) for axis-symmetric shapes [4], and random hyper-surface model (RHM) [5], Gaussian process (GP) [6], B-splines [7], and level-set RHM for arbitrary star-convex shapes [8]. Besides, the variational Bayesian inference is used as a powerful tool to yield a recursive expression due to the absence of conjugate prior [9]–[11].

Since the multi-agent systems have an appealing merit over the single agent for overcoming single-point failure, there has been a concerted effort to develop the system [12]. In [13], the weighted Kullback-Leibler divergence was applied to generate a consensus estimate. In [14], Hua *et al.* proposed a distributed filter with unknown prior information, and [15] provided a manner to fit the asynchronous fusion scenario. Considering that the MEM decomposes the extent into a parameterized vector, a diffusion filter was developed in [16] where each variable has an individual uncertainty instead a single value as in the RM. To enable a tracker still working properly when an object is detected by some specific sensor during every scan time, Li *et al.* proposed several distributed information filters over a general sensor network [17], [18]. These trackers further pave the way for some realistic engineering applications.

For most object types such as vehicles, the measurements (scattering source) distribute on the side visible to the sensor instead an uniform distribution across the extent (see, e.g., the nuScenes dataset [19]). To match the actual scenario, the method in [20] used a learned variational model on radar data, conducting the update using a particle filter. Xia *et al.* used the truncated Gaussian to describe the distribution of multiple measurements [21]. With this model, they calculate the mean and spread of augmented measurements by combining the pseudo-measurements lying on the truncated area with the raw measurements to yield a closed-form solution within the RM framework. In [22], a Gaussian mixture model was used to describe the measurement distribution, which was then reduced into a single Gaussian via moment matching. However, the existing tracking approaches ignore the inner correlation between the orientation and velocity, which causes the EOT merely being a joint estimation problem. In fact, a tracker will generate a decreased tracking error if it uses the correlation to update the unknown states as discussed in [23], [24].

In this work, we propose a novel state-coupled model (SCM) where the extent is described as the orientation and lengths of major axis and minor axis. Such a parametrization way completely determines the original extent if it is an axis-symmetric shape, such as an ellipse or rectangle. The orientation and velocity in SCM is treated as two coupled variables by introducing a sideslip angle. Meanwhile, the model assists a Gaussian Mixture distribution (GMD) to describe the bias towards the side of an object's extent visible to the sensor. To get an analytical expression in the measurement update stage, we use the deterministic sampling approach to estimate the kinematics and orientation information (includes a projection into the constraint space), and update the extent parameters in a Bayesian framework with pseudo-measurements. With these results, a simple moment matching technique is used to handle the GM reduction, yielding a single Gaussian distribution for recursive inference. The main difference to the models given in [23], [24] is that we use a GMD to handle the mismatch issue between the actual measurement distribution and theoretical hypothesis.

The contributions of this work are

- We give a novel state-coupled model (SCM) to establish a tight relation between the orientation and velocity vector. Therein, the distribution of measurements is

[1]Z. Li, S. Ma and H. Wang are with School of Space Information, Space Engineering University, Beijing 101416, China lee@seu.email.cn, shulima63@163.com and yhgnaw@163.com

[2]C. Liu is with College of Electronic Engineering, National University of Defense Technology, Hefei 230037, China liuchunsheng17a@nudt.edu.cn

modeled via a Gaussian mixture model.

- To generate an analytical expression for an update, we stack the kinematics, additive noise and multiplicative noise into a vector, and estimate them via a deterministic sampling approach, followed by a constraint condition. And the semi-lengths of object is estimated in a Bayesian framework with pseudo-measurements.
- Numerical simulations plus theoretical analysis verify the effectiveness of the proposed model and filter.

The remainder of the work is organized as follows. Section II gives a brief problem formulation. Section III gives an analytical solution for SCM. Section IV collects the proposed filter. Experimental examples are presented in Section V. Section VI concludes this work.

II. Problem Formulation

Here, we describe the proposed SCM, including state parameterization, measurement model, and evolution models.

A. State Parameterization

At time k, the following state vector $\boldsymbol{x}_k$ is considered

$$\boldsymbol{x}_k = [(\boldsymbol{x}_k^{\mathrm{c}})^{\mathsf{T}}, (\boldsymbol{x}_k^{\mathrm{s}})^{\mathsf{T}}]^{\mathsf{T}}, \tag{1}$$

where the kinematic state $\boldsymbol{x}_k^{\mathrm{c}}$

$$\boldsymbol{x}_k^{\mathrm{c}} = [x_k, y_k, v_k^{\mathsf{x}}, v_k^{\mathsf{y}}, \cdots]^{\mathsf{T}} \tag{2}$$

contains the Cartesian position $[x_k, y_k]^{\mathsf{T}} := \boldsymbol{m}_k$, velocity $[v_k^{\mathsf{x}}, v_k^{\mathsf{y}}]^{\mathsf{T}} := \boldsymbol{\vartheta}_k$ in x and y axes, and possible variables such as acceleration.

The angle vector $\boldsymbol{x}_k^{\mathrm{s}}$ includes

$$\boldsymbol{x}_k^{\mathrm{s}} = [p_k, q_k]^{\mathsf{T}}, \tag{3}$$

where $p_k = \cos(\beta_k)$ and $q_k = \sin(\beta_k)$ with $\beta_k := \arctan(\frac{v_k^{\mathsf{y}}}{v_k^{\mathsf{x}}}) - \alpha_k$ being the sideslip angle that represents a drift between the orientation α_k and velocity direction $\arctan(\frac{v_k^{\mathsf{y}}}{v_k^{\mathsf{x}}})$ [23], [24]. The extent parameters

$$\boldsymbol{l}_k = [l_{k,1}, l_{k,2}]^{\mathsf{T}}, \tag{4}$$

involve the semi-lengths $l_{k,1}$ and $l_{k,2}$.

B. Measurement Model

At time k, a sensor receives n_k Cartesian position measurements $\{\boldsymbol{y}_k^i\}_{i=1}^{n_k}$. Each individual scattering source $\boldsymbol{z}_k^i$ plus an addictive noise $\boldsymbol{v}_k^i \sim \mathcal{N}(\mathbf{0}, \mathbf{P}_v^i)$ generates the raw measurement $\boldsymbol{y}_k^i$ as shown in (5). Fig. 1 gives an illustration.

As pointed out in [22], real scattering source $\boldsymbol{z}_k^i$ is typically distributed at the sides of an object's extent visible to the sensor or at certain reflection region. Therefore, we introduce a GMD to model $\boldsymbol{z}_k^i$. Therein, the multiplicative noise $\boldsymbol{h}_k$ (the index i is omitted for simplicity)

$$\boldsymbol{h}_k \sim \sum_{j=1}^{J} \omega_j \mathcal{N}(\boldsymbol{h}_k^j; \bar{\boldsymbol{h}}_k^j, \mathbf{P}_h^j), \tag{7}$$

including J Gaussian mixture components with the corresponding weights $\omega_j, j = 1, 2, \cdots, J$, plays a vital role to match the actual distribution. With above analysis, we have the likelihood w.r.t $\boldsymbol{y}_k^i$

$$p(\boldsymbol{y}_k^i | \boldsymbol{x}_k, \boldsymbol{l}_k) = \sum_{j=1}^{J} \omega_j \mathcal{N}(\boldsymbol{y}_k^i; \mathbf{H}_k \boldsymbol{x}_k + \mathbf{S}_k \bar{\boldsymbol{h}}_j, \mathbf{S}_k \mathbf{P}_h^j \mathbf{S}_k^{\mathsf{T}} + \mathbf{P}_v^i). \tag{8}$$

C. Evolution Models

The temporal evolution models for the state vector and extent parameters are given as follows:

$$\boldsymbol{x}_{k+1} = \boldsymbol{\Phi}_k^x \boldsymbol{x}_k + \boldsymbol{w}_k^x \tag{9a}$$

$$\boldsymbol{l}_{k+1} = \boldsymbol{\Phi}_k^l \boldsymbol{l}_k + \boldsymbol{w}_k^l \tag{9b}$$

where $\boldsymbol{\Phi}_k^x$ and $\boldsymbol{\Phi}_k^l$ are transition matrices, $\boldsymbol{w}_k^x$ and $\boldsymbol{w}_k^l$ are zero-mean Gaussian process noises with covariances $\mathbf{P}_w^x$ and $\mathbf{P}_w^l$, respectively.

III. Closed-form Solution for Gaussian Mixture Distribution

A. Time Prediction

By equation (9), the predicted mean and error covariance are given as:

$$\hat{\boldsymbol{x}}_{k|k-1} = \boldsymbol{\Phi}_{k-1}^x \hat{\boldsymbol{x}}_{k-1|k-1}, \tag{10a}$$

$$\mathbf{P}_{x,k|k-1} = \boldsymbol{\Phi}_{k-1}^x \, \mathbf{P}_{x,k-1|k-1} \, (\boldsymbol{\Phi}_{k-1}^x)^{\mathsf{T}} + \mathbf{P}_w^x, \tag{10b}$$

$$\hat{\boldsymbol{l}}_{k|k-1} = \boldsymbol{\Phi}_{k-1}^l \hat{\boldsymbol{l}}_{k-1|k-1}, \tag{10c}$$

$$\mathbf{P}_{l,k|k-1} = \boldsymbol{\Phi}_{k-1}^l \, \mathbf{P}_{l,k-1|k-1} \, (\boldsymbol{\Phi}_{k-1}^l)^{\mathsf{T}} + \mathbf{P}_w^l. \tag{10d}$$

$$\boldsymbol{y}_k^i = \mathbf{H}_k \boldsymbol{x}_k + \underbrace{\begin{bmatrix} \frac{v_k^{\mathsf{y}} \sin\beta_k + v_k^{\mathsf{x}} \cos\beta_k}{\|\boldsymbol{\vartheta}_k\|} & \frac{v_k^{\mathsf{x}} \sin\beta_k - v_k^{\mathsf{y}} \cos\beta_k}{\|\boldsymbol{\vartheta}_k\|} \\ \frac{v_k^{\mathsf{y}} \cos\beta_k - v_k^{\mathsf{x}} \sin\beta_k}{\|\boldsymbol{\vartheta}_k\|} & \frac{v_k^{\mathsf{y}} \sin\beta_k + v_k^{\mathsf{x}} \cos\beta_k}{\|\boldsymbol{\vartheta}_k\|} \end{bmatrix} \begin{bmatrix} l_{k,1} & 0 \\ 0 & l_{k,2} \end{bmatrix}}_{:=\mathbf{S}_k} \underbrace{\begin{bmatrix} h_{k,1}^i \\ h_{k,2}^i \end{bmatrix}}_{:=\boldsymbol{h}_k^i} + \boldsymbol{v}_k^i \tag{5}$$

$$:= f(\boldsymbol{x}_k, \boldsymbol{l}_k, \boldsymbol{h}_k^i, \boldsymbol{v}_k^i) \tag{6}$$

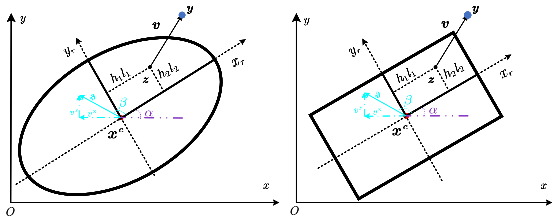

Fig. 1: An illustration of the model (5). For clarity, we omit the time index k and measurement index i in the figure. The Cartesian position is $\boldsymbol{m}$, and the extent and velocity are denoted as $\boldsymbol{l} = [l_1, l_2]^{\mathsf{T}}$ and $\boldsymbol{\vartheta} = [v^{\mathsf{x}}, v^{\mathsf{y}}]^{\mathsf{T}}$, respectively. By counterclockwise rotating an angle $\alpha = \arctan(v^{\mathsf{y}}/v^{\mathsf{x}})$ (i.e., the orientation) along x-axis, we get a reference frame x_r-y_r. The measurement source $\boldsymbol{z}$ is related to $\boldsymbol{l}$, $\boldsymbol{m}$ and $\boldsymbol{h} = [h_1, h_2]^{\mathsf{T}}$. The measurement $\boldsymbol{y}$ is the source $\boldsymbol{z}$ corrupted with a Gaussian noise $\boldsymbol{v}$.

B. Measurement Update

The measurement set $\{\boldsymbol{y}_k^i\}_{i=1}^{n_k}$ is processed sequentially in the measurement update stage. Let $\hat{\boldsymbol{x}}_{k|k}^{(i-1)}$, $\hat{\boldsymbol{l}}_{k|k}^{(i-1)}$, $\mathbf{P}_{x,k|k}^{(i-1)}$, and $\mathbf{P}_{l,k|k}^{(i-1)}$ denote the estimates and corresponding error covariances on the state vector and extent parameters, respectively, at the $(i-1)$-th processing. To start, the notation $\bullet_{k|k}^{(0)}$ corresponds to the predicted estimates. Since each individual measurement $\boldsymbol{y}_k^i, i \in \{1, \cdots n_k\}$, is related to a GMD, the updated value will leave us with J mixture components.

1) State Vector Update: Since the model (5) is highly nonlinear, we employ the deterministic sampling approach (DSA) (e.g., Unscented transform or Cubature transform) using a set of point masses $\boldsymbol{x}_k^{a,n}, n = 1, 2, \cdots, N$, with the corresponding weights $\alpha_k^n, n = 1, 2, \cdots, N$ to approximate the mean and covariance of $f(\boldsymbol{x}_k^a)$ [25], [26], where the extent parameters $\boldsymbol{l}_k$ are replaced by their estimates. To this end, we first augment the original state $\boldsymbol{x}_k$ as

$$\boldsymbol{x}_k^a = \left[(\boldsymbol{x}_k)^{\mathsf{T}}, (\boldsymbol{h}_k^j)^{\mathsf{T}}, (\boldsymbol{v}_k^i)^{\mathsf{T}}\right]^{\mathsf{T}} \tag{11}$$

with the augmented measurement $\boldsymbol{y}_k^a = [\boldsymbol{y}_k^i, 1]^{\mathsf{T}}$. Then, we have

$$\begin{aligned}(\bar{\boldsymbol{y}}_{k|k-1}^a, \mathbf{C}_k^y, \mathbf{C}_k^{xy}) &= \mathrm{DSA}\left[\langle f(\boldsymbol{x}_k^a), 1\rangle, \bar{\boldsymbol{x}}_{k|k-1}^a, \mathbf{P}_{x,k|k-1}^a\right] \\ &= \mathrm{DSA}\Bigg[\left\langle f(\boldsymbol{x}_k, \boldsymbol{h}_k^j, \boldsymbol{v}_k^i), 1\right\rangle, \left((\hat{\boldsymbol{x}}_{k|k-1})^{\mathsf{T}}, (\bar{\boldsymbol{h}}_k^j)^{\mathsf{T}}, \mathbf{0}_{2\times1}^{\mathsf{T}}\right)^{\mathsf{T}}, \\ &\qquad \mathrm{diag}(\mathbf{P}_{x,k|k-1}, \mathbf{P}_h^j, \mathbf{P}_v^i)\Bigg]\end{aligned} \tag{12}$$

where

$$\bar{\boldsymbol{y}}_{k|k-1}^a = \sum_{n=1}^N \alpha_k^n \boldsymbol{y}_k^{a,n}, \boldsymbol{y}_k^{a,n} = f(\boldsymbol{x}_k^{a,n}), \tag{13a}$$

$$\mathbf{C}_k^y = \sum_{n=1}^N \alpha_k^n (\bar{\boldsymbol{y}}_{k|k-1}^a - \boldsymbol{y}_k^{a,n})(\bar{\boldsymbol{y}}_{k|k-1}^a - \boldsymbol{y}_k^{a,n})^{\mathsf{T}}, \tag{13b}$$

$$\mathbf{C}_k^{xy} = \sum_{n=1}^N \alpha_k^n (\hat{\boldsymbol{x}}_{k|k-1} - \boldsymbol{x}_k^n)(\bar{\boldsymbol{y}}_{k|k-1}^a - \boldsymbol{y}_k^{a,n})^{\mathsf{T}}. \tag{13c}$$

with $\boldsymbol{x}_k^n, n = 1, 2, \cdots, N$, being the truncated portion of $\boldsymbol{x}_k^{a,n}$ to match the dimension of $\boldsymbol{x}_k$.

With above analysis, we get

$$\mathbf{K}_k = \mathbf{C}_k^{xy}/\mathbf{C}_k^y, \tag{14a}$$

$$\hat{\boldsymbol{x}}_{k|k}^{j,(i)} = \hat{\boldsymbol{x}}_{k|k}^{(i-1)} + \mathbf{K}_k(\boldsymbol{y}_k^a - \bar{\boldsymbol{y}}_{k|k-1}^a), \tag{14b}$$

$$\mathbf{P}_{x,k|k}^{j,(i)} = \mathbf{P}_{x,k|k}^{(i-1)} + \mathbf{K}_k \mathbf{C}_k^y (\mathbf{K}_k)^{\mathsf{T}}. \tag{14c}$$

Note that each sequential update will generate J mixture components, i.e., after the updating with measurement $\boldsymbol{y}_k^i$, we get

$$p(\boldsymbol{x}_k^{(i)}|\boldsymbol{y}_k^i) = \sum_{j=1}^J \omega_j^+ \mathcal{N}\left(\boldsymbol{x}_k^{(i)}; \hat{\boldsymbol{x}}_{k|k}^{j,(i)}, \mathbf{P}_{x,k|k}^{j,(i)}\right) \tag{15}$$

where $\omega_j^+ = \omega_j \cdot l_j^y$ is the updated weight with l_j^y being the likelihood function related the j-th component of $\boldsymbol{h}_k$.

To reduce the GMD to a single Gaussian after the sequential processing, we use the moment matching technique to yield the final expressions

$$\hat{\boldsymbol{x}}_{k|k}^{(i)} = \sum_{j=1}^J \frac{\omega_j^+}{\sum_{j=1}^J \omega_j^+} \hat{\boldsymbol{x}}_{k|k}^{j,(i)}, \tag{16a}$$

$$\begin{aligned}\mathbf{P}_{x,k|k}^{(i)} = \sum_{j=1}^J \frac{\omega_j^+}{\sum_{j=1}^J \omega_j^+} \Big(&\mathbf{P}_{x,k|k}^{j,(i)} \\ &+ \left(\hat{\boldsymbol{x}}_{k|k}^{(i)} - \hat{\boldsymbol{x}}_{k|k}^{j,(i)}\right)\left(\hat{\boldsymbol{x}}_{k|k}^{(i)} - \hat{\boldsymbol{x}}_{k|k}^{j,(i)}\right)^{\mathsf{T}}\Big).\end{aligned} \tag{16b}$$

2) Extent Parameters Update: the pseudo-measurement (corresponds to the j-th component) is

$$\mathbf{Y}_k^{j,i} = \mathbf{F}\left((\boldsymbol{y}_k^i - \bar{\boldsymbol{y}}_k^j) \otimes (\boldsymbol{y}_k^i - \bar{\boldsymbol{y}}_k^j)\right), \tag{17}$$

with

$$\bar{\boldsymbol{y}}_k^j = \mathbf{H}_k \hat{\boldsymbol{x}}_{k|k}^{(i-1)} + \hat{\mathbf{S}}_k^{(i-1)} \bar{\boldsymbol{h}}_k^j. \tag{18}$$

The expected value and covariance of the i-th pseudo-measurement related to the j-th component are

$$\bar{\mathbf{Y}}_k^{j,i} = \mathbf{F} \cdot \mathrm{vect}(\mathbf{P}_k^{y,j}), \tag{19a}$$

$$\mathbf{P}_k^{Y,j} = \mathbf{F}(\mathbf{P}_k^{y,j} \otimes \mathbf{P}_k^{y,j})(\mathbf{F} + \tilde{\mathbf{F}})^{\mathsf{T}}, \tag{19b}$$

where the notation $\mathrm{vect}(\cdot)$ reshapes a matrix into a new vector by stacking all the columns of the matrix, and the cross-covariance between the pseudo-measurement and extent parameters is

$$\mathbf{P}_k^{lY,j} = \mathbf{P}_{l,k|k}^{(i-1)} \mathbf{M}_k^j, \tag{20}$$

where

$$\mathbf{P}_k^{y,j} = \mathbf{H}_k \mathbf{P}_{x,k|k}^{(i-1)} \mathbf{H}_k^{\mathsf{T}} + \mathbf{P}^{\mathrm{I}} + \mathbf{P}^{\mathrm{II}} + \mathbf{P}^{\mathrm{III}} + \mathbf{P}_v^i, \tag{21}$$

$$\mathbf{F} = \begin{bmatrix} 1 & 0 & 0 & 0 \\ 0 & 0 & 0 & 1 \\ 0 & 1 & 0 & 0 \end{bmatrix}, \tilde{\mathbf{F}} = \begin{bmatrix} 1 & 0 & 0 & 0 \\ 0 & 0 & 0 & 1 \\ 0 & 0 & 1 & 0 \end{bmatrix}, \tag{22}$$

with

$$\mathbf{M}_k^j = \begin{bmatrix} 2\hat{\mathbf{S}}_{k,1}^{(i-1)}\mathbf{P}_h^j\hat{\mathbf{J}}_{1k,l}^{(i-1)} \\ 2\hat{\mathbf{S}}_{k,2}^{(i-1)}\mathbf{P}_h^j\hat{\mathbf{J}}_{2k,l}^{(i-1)} \\ \hat{\mathbf{S}}_{k,1}^{(i-1)}\mathbf{P}_h^j\hat{\mathbf{J}}_{1k,l}^{(i-1)} + 2\hat{\mathbf{S}}_{k,2}^{(i-1)}\mathbf{P}_h^j\hat{\mathbf{J}}_{2k,l}^{(i-1)} \end{bmatrix}, \tag{23a}$$

$$\mathbf{P}^{\mathrm{I}} = \hat{\mathbf{S}}_k^{(i-1)}\mathbf{P}_h^j\left(\hat{\mathbf{S}}_k^{(i-1)}\right)^\top, \tag{23b}$$

$$\underbrace{[\epsilon_{mn}]}_{\mathbf{P}^{\mathrm{II}}} = \mathrm{tr}\left\{\mathbf{P}_{l,k|k}^{(i-1)}\left(\hat{\mathbf{J}}_{nk,l}^{(i-1)}\right)^\top(\mathbf{P}_h^j + \bar{\boldsymbol{h}}_k^j(\bar{\boldsymbol{h}}_k^j)^\top)\hat{\mathbf{J}}_{mk,l}^{(i-1)}\right\}, \tag{23c}$$

$$\underbrace{[\varpi_{mn}]}_{\mathbf{P}^{\mathrm{III}}} = \mathrm{tr}\left\{\mathbf{P}_{x,k|k}^{(i-1)}\left(\hat{\mathbf{J}}_{nk,x}^{(i-1)}\right)^\top(\mathbf{P}_h^j + \bar{\boldsymbol{h}}_k^j(\bar{\boldsymbol{h}}_k^j)^\top)\hat{\mathbf{J}}_{mk,x}^{(i-1)}\right\}, \tag{23d}$$

for the entry indexes $m, n \in \{1, 2\}$. Here, $\hat{\bullet}^{(i-1)}$ represents the variable $\bullet$ obtained based on the $(i-1)$-th estimate.

Proof: Detailed derivation of (21) is given in Appendix. ■

Then, we have

$$\hat{\boldsymbol{l}}_{k|k}^{j,(i)} = \hat{\boldsymbol{l}}_{k|k}^{(i-1)} + \mathbf{P}_k^{lY,j}/\mathbf{P}_k^{Y,j}(\mathbf{Y}_k^{j,i} - \bar{\mathbf{Y}}_k^{j,i}), \tag{24a}$$

$$\mathbf{P}_{l,k|k}^{j,(i)} = \mathbf{P}_{l,k|k}^{(i-1)} + \mathbf{P}_k^{lY,j}/\mathbf{P}_k^{Y,j}(\mathbf{P}_k^{lY,j})^\top. \tag{24b}$$

The final estimates on extent parameters $\boldsymbol{l}$ are handled similarly as in $\boldsymbol{x}$.

IV. Implementation

A. Constrained Estimation

Clearly, the two variables p_k and q_k in (3) have such a relation

$$p_k^2 + q_k^2 = 1. \tag{25}$$

We rewrite (25) as

$$([\mathbf{0}_{2\times 4}, \mathbf{I}_2]\boldsymbol{x}_k)^\top([\mathbf{0}_{2\times 4}, \mathbf{I}_2]\boldsymbol{x}_k) = 1 \tag{26}$$

where $\mathbf{I}_2$ and $\mathbf{0}_{2\times 4}$ are full zero and identity matrices with the appropriate dimension, respectively. Then (26) can be written as

$$(\boldsymbol{x}_k)^\top\mathbf{D}\boldsymbol{x}_k = 1 \tag{27}$$

where $\mathbf{D} = \mathrm{diag}(0, 0, 0, 0, 1, 1)$. Based on the constraint condition (27), we project $\hat{\boldsymbol{x}}_{k|k}$ into the constraint space to get the solution of the optimization function (28)

$$\begin{aligned} &\arg\min_{\boldsymbol{c}}(\boldsymbol{c} - \hat{\boldsymbol{x}}_{k|k})^\top\mathbf{W}_k(\boldsymbol{c} - \hat{\boldsymbol{x}}_{k|k}) \\ &\text{s.t.} \quad \boldsymbol{c}^\top\mathbf{D}\boldsymbol{c} = 1 \end{aligned} \tag{28}$$

where $\mathbf{W}_k$ is selected as $\mathbf{P}_{x,k|k}$.

Since (28) is non-convex w.r.t $\boldsymbol{c}$, we perform first order series expansion, yielding

$$\boldsymbol{c}^\top\mathbf{D}\boldsymbol{c} \approx (\hat{\boldsymbol{x}}_{k|k})^\top\mathbf{D}\hat{\boldsymbol{x}}_{k|k} + (2\mathbf{D}\hat{\boldsymbol{x}}_{k|k})^\top(\boldsymbol{c} - \hat{\boldsymbol{x}}_{k|k}). \tag{29}$$

Then, the constrained estimate $\hat{\boldsymbol{x}}_{k|k}^p$ and its error covariance are given as

$$\begin{aligned} \hat{\boldsymbol{x}}_{k|k}^p = \hat{\boldsymbol{x}}_{k|k} &+ \mathbf{P}_{x,k|k}(2\mathbf{D}\hat{\boldsymbol{x}}_{k|k})/(2\mathbf{D}\hat{\boldsymbol{x}}_{k|k})^\top\mathbf{P}_{x,k|k}(2\mathbf{D}\hat{\boldsymbol{x}}_{k|k}) \\ &\times\left[1 - (\hat{\boldsymbol{x}}_{k|k})^\top\mathbf{D}\hat{\boldsymbol{x}}_{k|k}\right] \end{aligned} \tag{30a}$$

$$\mathbf{P}_{k|k}^p = \mathbf{B}\mathbf{P}_{x,k|k}\mathbf{B}^\top \tag{30b}$$

where

$$\begin{aligned} \mathbf{B} = \mathbf{I} - &\mathbf{P}_{x,k|k}(\mathbf{D}\hat{\boldsymbol{x}}_{k|k}) \\ &\times\left[(\mathbf{D}\hat{\boldsymbol{x}}_{k|k})^\top\mathbf{P}_{x,k|k}(\mathbf{D}\hat{\boldsymbol{x}}_{k|k})\right]^{-1}(\mathbf{D}\hat{\boldsymbol{x}}_{k|k})^\top. \end{aligned} \tag{31}$$

B. Parameters Calculation

In general, the weights and components need to be estimated or learned by using a large amount of data. In this work, we choose four components

$$\bar{\boldsymbol{h}} = \begin{bmatrix} 0.8 & 0 & -0.8 & 0 \\ 0 & 0.8 & 0 & -0.8 \end{bmatrix} \tag{32}$$

$$\mathbf{P}_h = \begin{bmatrix} \mathrm{diag}(\frac{1}{200} \quad \frac{1}{3}) \\ \mathrm{diag}(\frac{1}{3} \quad \frac{1}{200}) \\ \mathrm{diag}(\frac{1}{200} \quad \frac{1}{3}) \\ \mathrm{diag}(\frac{1}{3} \quad \frac{1}{200}) \end{bmatrix} \tag{33}$$

to approximate the GMD of a rectangular shape [22]. And the entry $\frac{1}{3}$ in $\mathbf{P}_h$ is replaced by $\frac{1}{4}$ for an ellipse. To fit most tracking scenarios, the weights are set to be different values according to the geometry between the sensor and object. In detail, the weight is higher when an object moves toward the sensor and lower weight, otherwise [22]. The required weights are given as follows:

$$\begin{cases} \omega_j = 0.9, & \text{if } \theta_j < 0.4\pi \\ \omega_j = 0.5, & \text{if } 0.4\pi \leq \theta_j < 0.7\pi \\ \omega_j = 0.001, & \text{else} \end{cases}, \tag{34a}$$

$$\theta_j = \left|(\measuredangle(\boldsymbol{s}_x) - \measuredangle(\bar{\boldsymbol{h}}^j) + \pi, \mod 2\pi) - \pi\right|, \tag{34b}$$

$$\boldsymbol{s}_x = \mathrm{diag}\begin{pmatrix} \frac{1}{l_1} & \frac{1}{l_2} \end{pmatrix} \cdot \mathbf{R}_\alpha^\top \cdot (\boldsymbol{s} - \boldsymbol{m}), \tag{34c}$$

where $\boldsymbol{s}_x$ transforms the sensor's position $\boldsymbol{s}$ into the unit coordinates, $\mathbf{R}_\alpha$ is the rotation matrix related to the orientation α, and the notation $\measuredangle(\cdot)$ returns the corresponding angle [22]. The filter so-called Gaussian Mixture Distribution-State-Coupled Model (GMD-SCM) is summarized in Algorithm 1.

V. Numerical Examples

In this section, we compare the proposed GMD-SCM filter with GMD-MEM filter [22] (abbreviated as SCM and MEM, respectively) and CVM filter with a single node [24] over 3 different dynamic scenarios. We evaluate the estimation errors by the Gaussian Wasserstein distance (GWD) for assessing both the position and extent errors over $M = 50$ Monte Carlo runs [4].

Initialization: $\hat{\boldsymbol{x}}^{(0)}_{1|0}$, $\hat{\boldsymbol{l}}^{(0)}_{1|0}$, $\mathbf{P}^{(0)}_{x,1|0}$, and $\mathbf{P}^{(0)}_{l,1|0}$;
for $k \leftarrow 1, 2, \cdots$ `// scan time` **do**
  Data: $\{\boldsymbol{y}^i_k\}_{i=1}^{n_k}$;
  for $j = 0, \cdots, J-1$ **do**
    $\omega_j \leftarrow$ using $\boldsymbol{s}_x$ and $\boldsymbol{h}^j$
  end
  for $i = 1, 2, \cdots, n_k$ `// sequential` **do**
    for $j = 0, \cdots, J-1$ `// mixture` **do**
      $\hat{\boldsymbol{x}}^{j,(i)}_{k|k}, \mathbf{P}^{j,(i)}_{x,k|k}, \hat{\boldsymbol{l}}^{j,(i)}_{k|k}, \mathbf{P}^{j,(i)}_{l,k|k}, l^y_j \leftarrow$ `Update` $\hat{\boldsymbol{x}}^{(i-1)}_{k|k}, \mathbf{P}^{(i-1)}_{x,k|k}, \hat{\boldsymbol{l}}^{(i-1)}_{k|k}, \mathbf{P}^{(i-1)}_{l,k|k}$ via (14) and (24);
      $\omega^+_j \leftarrow \omega_j \cdot l^y_j$;
    end
    $\omega^+_j \leftarrow$ `Normalize` ω^+_j ;
    $\hat{\boldsymbol{x}}^{(i)}_{k|k}, \mathbf{P}^{(i)}_{x,k|k} \leftarrow$ (16) using all $\omega^+_j, \hat{\boldsymbol{x}}^{j,(i)}_{k|k}, \mathbf{P}^{j,(i)}_{x,k|k}$;
    $\hat{\boldsymbol{l}}^{(i)}_{k|k}, \mathbf{P}^{(i)}_{l,k|k} \leftarrow$ (16) using all $\omega^+_j, \hat{\boldsymbol{l}}^{j,(i)}_{k|k}, \mathbf{P}^{j,(i)}_{l,k|k}$;
  end
  Return1: $\hat{\boldsymbol{x}}_{k|k} \leftarrow \hat{\boldsymbol{x}}^{(n_k)}_{k|k}, \mathbf{P}_{x,k|k} \leftarrow \mathbf{P}^{(n_k)}_{x,k|k}$;
  $\hat{\boldsymbol{x}}^p_{k|k}, \mathbf{P}^p_{x,k|k} \leftarrow$ `Project` $\hat{\boldsymbol{x}}_{k|k}, \mathbf{P}_{x,k|k}$ via (30) ;
  Return2: $\hat{\boldsymbol{l}}_{k|k} \leftarrow \hat{\boldsymbol{l}}^{(n_k)}_{k|k}, \mathbf{P}_{l,k|k} \leftarrow \mathbf{P}^{(n_k)}_{l,k|k}$;
  $\hat{\boldsymbol{x}}_{k+1|k}, \mathbf{P}_{x,k+1|k}, \hat{\boldsymbol{l}}_{k+1|k}, \mathbf{P}_{l,k+1|k} \leftarrow$ `Prediction` $\hat{\boldsymbol{x}}^p_{k|k}, \mathbf{P}^p_{x,k|k}, \hat{\boldsymbol{l}}_{k|k}, \mathbf{P}_{l,k|k}$ via (10)
end

Algorithm 1: GMD-SCM Filter. The function `Update` gives the updated means and covariances of the state vector and extent parameters. The function `Normalize` normalizes the input weights. The function `Project` projects the state vector into the constraint space. The function `Prediction` gives the predicted means and covariances of the state vector and extent parameters.

A. Rectangular Object Moves Along the Orientation

In this scenario (S1), the considered object is a rectangle with lengths 3 and 4 meters. The orientation of the object is aligned with its direction of velocity. The parameters used in S1 are collected in Table I. Fig. 2 gives the true trajectory and whole tracking results. As shown in Fig. 2, the proposed SCM deals with such a situation more effectively since its estimates are closer to the ground truth than MEM and CVM at most time steps. The reason is twofold. On the one hand, SCM is capable of describing the correlation between the velocity and orientation, so SCM quickly modifies its filtering gain. On the other hand, SCM describes the actual received data distributed mainly on the side visible to the sensor. Fig. 3 shows the GWD distance, and its result verifies the advantage of SCM.

TABLE I: Parameters used in S1 & S2

Categories	Para.	Specification
Common	Scan Time	$T = 3$ s
	Sensor's Position	$\boldsymbol{s} = [0, 0]^{\mathrm{T}}$
	Mea. Cov.	$\mathbf{P}^i_v = \mathrm{diag}(\frac{1}{3}, \frac{1}{3})$
	No. of Meas.	$\lambda = 10$
MEM	Extent Transition Matrix	$\boldsymbol{\Phi}^l_k = \mathbf{I}_3$
	State Transition Matrix	$\boldsymbol{\Phi}^x_k = \begin{bmatrix} 1 & T \\ 0 & 1 \end{bmatrix} \otimes \mathbf{I}_2$
	Process Cov. in Extent	$\mathbf{P}^l_w = \mathrm{diag}(.01, .05^2, .05^2)$
	Cov. in Extent	$\mathbf{P}^{(0)}_{l,1\|0} = \mathrm{diag}(.01, \frac{1}{50}, \frac{1}{10})$
	Process Cov. in State	$\mathbf{P}^x_w = \mathrm{diag}(50, 50, 10, 10)$
	Cov. in State	$\mathbf{P}^{(0)}_{x,1\|0} = \mathrm{diag}(2, 2, \frac{1}{5}, \frac{1}{5})$
SCM	Extent Transition Matrix	$\boldsymbol{\Phi}^l_k = \mathbf{I}_2$
	State Transition Matrix	$\boldsymbol{\Phi}^x_k = \begin{bmatrix} 1 & T & 0 \\ 0 & 1 & 0 \\ 0 & 0 & 1 \end{bmatrix} \otimes \mathbf{I}_2$
	Process Cov. in Extent	$\mathbf{P}^l_w = \mathrm{diag}(.05^2, .05^2)$
	Cov. in Extent	$\mathbf{P}^{(0)}_{l,1\|0} = \mathrm{diag}(\frac{1}{50}, \frac{1}{10})$
	Process Cov. in State	$\mathbf{P}^x_w = \mathrm{diag}(50, 50, 10, 10, .01, .01)$
	Cov. in State	$\mathbf{P}^{(0)}_{x,1\|0} = \mathrm{diag}(2, 2, \frac{1}{5}, \frac{1}{5}, .01, .01)$

TABLE II: Parameters used in S3

Categories	Para.	Specification
Common	Mea. Cov.	$\mathbf{P}^i_v = \mathrm{diag}(50, 8)$
MEM	Process Cov. in Extent	$\mathbf{P}^l_w = \mathrm{diag}(.01, .05^2, .05^2)$
	Cov. in Extent	$\mathbf{P}^{(0)}_{l,1\|0} = \mathrm{diag}(.05, 10, 4)$
	Process Cov. in State	$\mathbf{P}^x_w = \mathrm{diag}(10^2, 10^2, 20, 20)$
	Cov. in State	$\mathbf{P}^{(0)}_{x,1\|0} = \mathrm{diag}(50, 50, 1, 1)$
SCM	Process Cov. in Extent	$\mathbf{P}^l_w = \mathrm{diag}(.05^2, .05^2)$
	Cov. in Extent	$\mathbf{P}^{(0)}_{l,1\|0} = \mathrm{diag}(10, 4)$
	Process Cov. in State	$\mathbf{P}^x_w = \mathrm{diag}(10^2, 10^2, 20, 20, .01, .01)$
	Cov. in State	$\mathbf{P}^{(0)}_{x,1\|0} = \mathrm{diag}(50, 50, 1, 1, .01, .01)$

B. Rectangular Object Moves with a Drift

In this scenario (S2), the considered object is a rectangle with lengths 3 and 4 meters. Its orientation is a constant value $\frac{\pi}{4}$, and it moves firstly with a drift and then goes with a turn. As depicted in Fig. 4, SCM that allows an object to do a drift motion keeps a better tracking results on the kinematics and extent parameters over most time steps, but MEM and CVM get worse after the object moves away from the sensor. From Fig. 5, we observe that SCM has an overall lower level GWD distance than MEM and CVM, which indicates the superiority on SCM.

C. Elliptical Object Moves Along the Orientation

In this scenario (S3), the considered object is an ellipse with lengths of the semi-axes 40 m and 20 m. Table II collects the parameters used in S3, and the other required parameters are given in Table I. Fig. 6 shows the overall tracking results. To provide a visible viewpoint, Fig. 7 gives the GWD distance. As expected, SCM has a lower error than MEM and CVM, as it treats the velocity and orientation as two dependent variables, followed an efficient GWD model. The facts in turn deliver a positive feedback to improve SCM's performance.

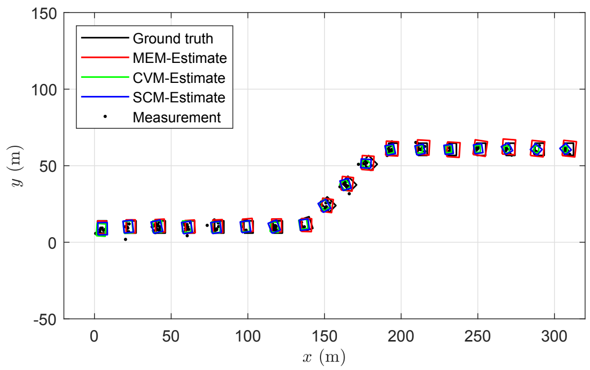

Fig. 2: Measurements, trajectory, and estimation results in S1

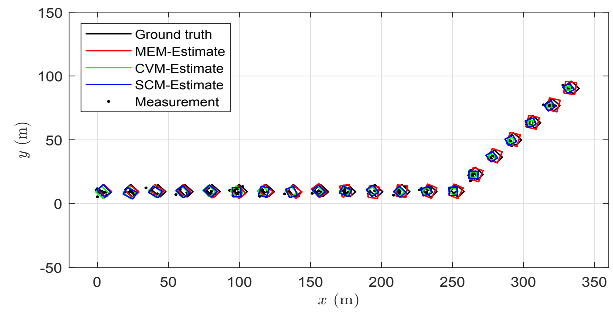

Fig. 4: Measurements, trajectory, and estimation results in S2

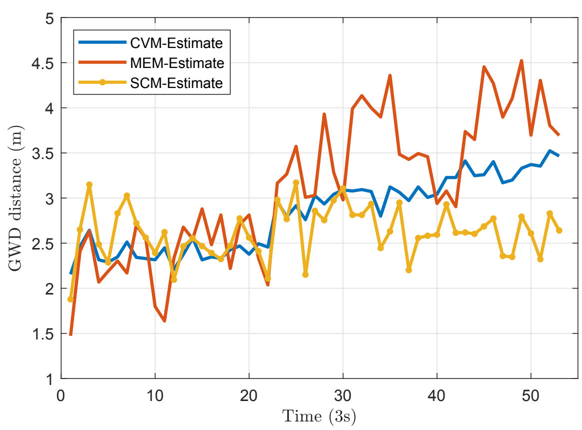

Fig. 3: GWDs with different filters in S1

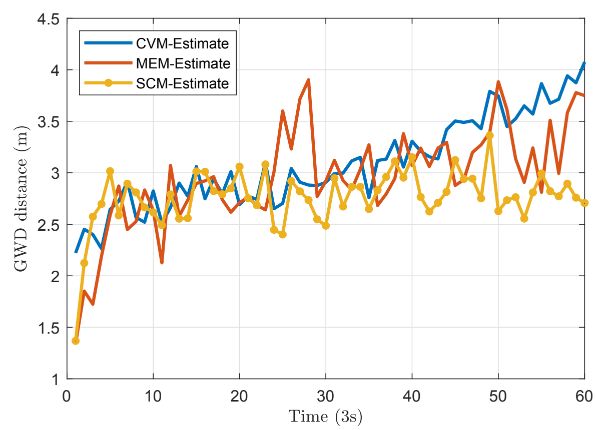

Fig. 5: GWDs with different filters in S2

VI. CONCLUSIONS

To describe the real measurements distributed on particular region of an object's extent, this work first proposes a novel state-coupled model with Gaussian mixture distribution. Meanwhile, the model considers the correlation between the orientation and velocity. We then derive a problem-tailored filter to generate a recursive solution by comprehensively using the deterministic sampling approach, moment matching and optimization method with constraint. Numerical results show that the proposed filter has an improved performance.

APPENDIX

Proof: For brevity, we first derive the partial derivatives as

$$\begin{cases} d_1 = \dfrac{\partial v_k^{\mathsf{x}}/\|\boldsymbol{\vartheta}_k\|}{\partial v_k^{\mathsf{x}}}\Bigg|_{\hat{\boldsymbol{\vartheta}}_{k|k}^{(i-1)}} = \dfrac{1}{\|\boldsymbol{\vartheta}_k\|} - \dfrac{(v_k^{\mathsf{x}})^2}{(\|\boldsymbol{\vartheta}_k\|)^3}\Bigg|_{\hat{\boldsymbol{\vartheta}}_{k|k}^{(i-1)}}, \\ d_2 = \dfrac{\partial v_k^{\mathsf{y}}/\|\boldsymbol{\vartheta}_k\|}{\partial v_k^{\mathsf{y}}}\Bigg|_{\hat{\boldsymbol{\vartheta}}_{k|k}^{(i-1)}} = \dfrac{1}{\|\boldsymbol{\vartheta}_k\|} - \dfrac{(v_k^{\mathsf{y}})^2}{(\|\boldsymbol{\vartheta}_k\|)^3}\Bigg|_{\hat{\boldsymbol{\vartheta}}_{k|k}^{(i-1)}}, \\ d_3 = \dfrac{\partial v_k^{\mathsf{y}}/\|\boldsymbol{\vartheta}_k\|}{\partial v_k^{\mathsf{x}}} = \dfrac{\partial v_k^{\mathsf{x}}/\|\boldsymbol{\vartheta}_k\|}{\partial v_k^{\mathsf{y}}}\Bigg|_{\hat{\boldsymbol{\vartheta}}_{k|k}^{(i-1)}} = -\dfrac{v_k^{\mathsf{x}} v_k^{\mathsf{y}}}{(\|\boldsymbol{\vartheta}_k\|)^3}\Bigg|_{\hat{\boldsymbol{\vartheta}}_{k|k}^{(i-1)}}. \end{cases} \tag{35}$$

Performing the first-order Taylor series expansion in term $\mathbf{S}_k \boldsymbol{h}_k^j$ around the $(i-1)$-th estimates $\hat{\boldsymbol{l}}_{k|k}^{(i-1)}$ and $\hat{\boldsymbol{x}}_{k|k}^{(i-1)}$, respectively, yields

$$\begin{aligned} \mathbf{S}_k \boldsymbol{h}_k^j \approx & \underbrace{\hat{\mathbf{S}}_k^{(i-1)} \boldsymbol{h}_k^j}_{\mathrm{I}} + \underbrace{\begin{bmatrix} \left(\boldsymbol{h}_k^j\right)^{\mathsf{T}} \hat{\mathbf{J}}_{1k,l}^{(i-1)} \\ \left(\boldsymbol{h}_k^j\right)^{\mathsf{T}} \hat{\mathbf{J}}_{2k,l}^{(i-1)} \end{bmatrix} \left(\boldsymbol{l}_k - \hat{\boldsymbol{l}}_{k|k}^{(i-1)}\right)}_{\mathrm{II}} \\ & + \underbrace{\begin{bmatrix} \left(\boldsymbol{h}_k^j\right)^{\mathsf{T}} \hat{\mathbf{J}}_{1k,x}^{(i-1)} \\ \left(\boldsymbol{h}_k^j\right)^{\mathsf{T}} \hat{\mathbf{J}}_{2k,x}^{(i-1)} \end{bmatrix} \left(\boldsymbol{x}_k - \hat{\boldsymbol{x}}_{k|k}^{(i-1)}\right)}_{\mathrm{III}} \end{aligned} \tag{36}$$

where $\hat{\mathbf{J}}_{1k,x}$ and $\hat{\mathbf{J}}_{2k,x}$ are the Jacobian matrices of the first row $\mathbf{S}_{1,k}$ and second row $\mathbf{S}_{2,k}$ of $\mathbf{S}_k$ at the $(i-1)$-th estimate $\hat{\boldsymbol{x}}_{k|k}^{(i-1)}$, respectively. And $\hat{\mathbf{J}}_{1k,l}$ and $\hat{\mathbf{J}}_{2k,l}$ are the Jacobian matrices of the first row $\mathbf{S}_{1,k}$ and second row $\mathbf{S}_{2,k}$ of $\mathbf{S}_k$ at the $(i-1)$-th estimate $\hat{\boldsymbol{l}}_{k|k}^{(i-1)}$, respectively. Substituting (36) and (7) into (5), using the fact that the terms II and III in (36) are scalar, then the residual covariance in $\boldsymbol{y}_k^i$ related to

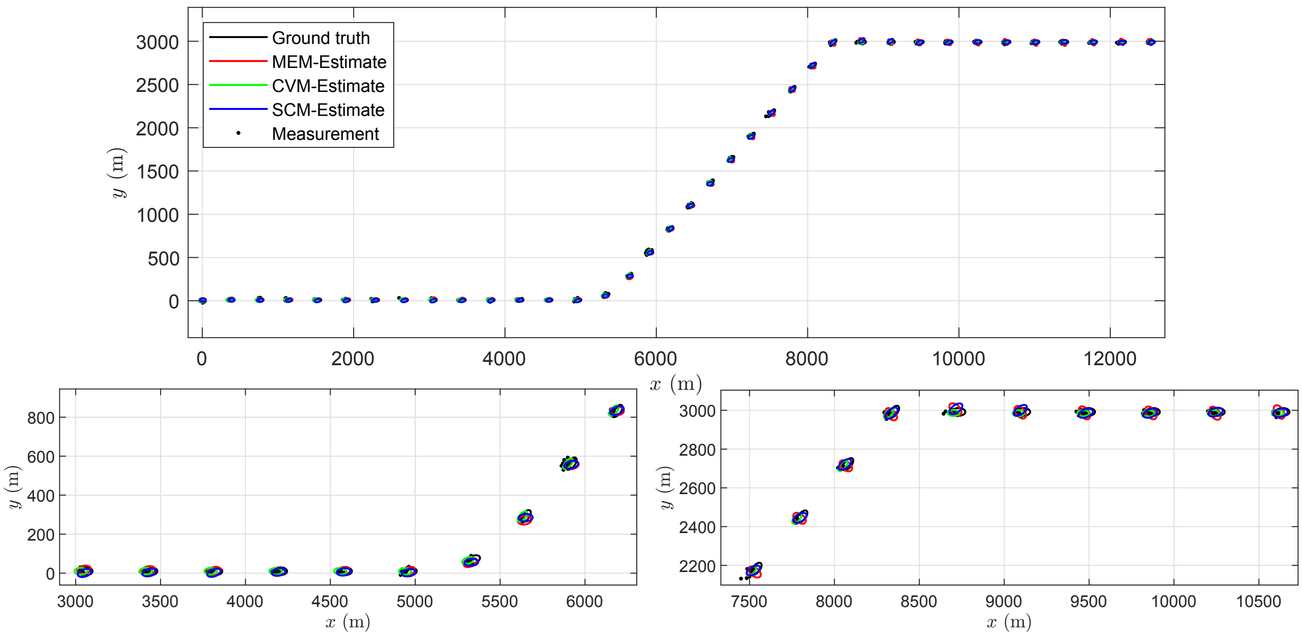

Fig. 6: Measurements, trajectory, and estimation results in S3

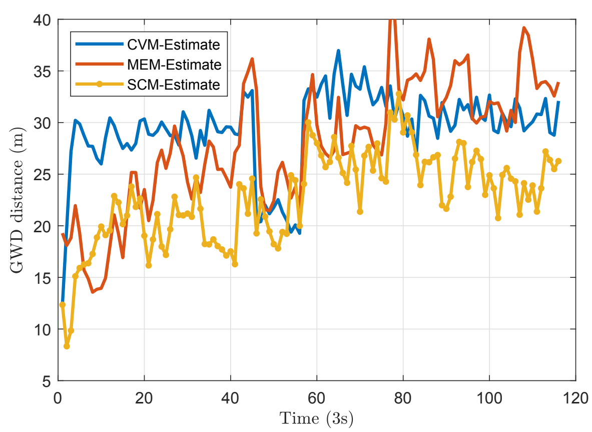

Fig. 7: GWDs with different filters in S3

the j-th component is given as

$$\mathbf{P}_k^{y,j} = \mathbf{H}_k \mathbf{P}_{x,k|k}^{(i-1)} \mathbf{H}_k^{\mathrm{T}} + \mathbf{P}^{\mathrm{I}} + \mathbf{P}^{\mathrm{II}} + \mathbf{P}^{\mathrm{III}} + \mathbf{P}_v^i. \quad (41)$$

■

References

[1] K. Granström and M. Baum, "A Tutorial on Multiple Extended Object Tracking," *techrxiv.19115858.v1*, 2022.

[2] K. Granström and J. Bramstång, "Bayesian Smoothing for the Extended Object Random Matrix Model,"*IEEE Trans. Signal Process.*, vol. 67, no. 14, pp. 3732-3742, 2019.

[3] J. Lan and X. R. Li, "Extended Object or Group Target Tracking Using Random Matrix with Nonlinear Measurements," *IEEE Trans. Signal Process.*, vol. 67, no. 19, pp. 5130-5142, 2019.

[4] S. Yang and M. Baum, "Tracking the Orientation and Axes Lengths of an Elliptical Extended Object," *IEEE Trans. Signal Process.*, vol.67, no.1, pp. 4720–4729, 2019.

[5] M. Baum and U. D. Hanebeck, "Shape Tracking of Extended Objects and Group Targets with Star-Convex RHMs," in *Proc. 14th Int. Conf. Inf. Fusion*, Chicago, IL, USA, July 2011, pp. 1-8.

[6] W. Aftab, R. Hostettler, A. De Freitas, M. Arvaneh and L. Mihaylova, "Spatio-Temporal Gaussian Process Models for Extended and Group Object Tracking with Irregular Shapes," *IEEE Trans. Veh. Technol.*, vol. 68, no. 3, pp. 2137-2151, 2019.

[7] H. Kaulbersch, J. Honer and M. Baum, "A Cartesian B-Spline Vehicle Model for Extended Object Tracking," in *Proc. 2018 21st Int. Conf. Inf. Fusion*, Cambridge, UK, July 2018, pp. 1-5.

[8] A. Zea, F. Faion, M. Baum and U. D. Hanebeck, "Level-Set Random Hyper-Surface Models for Tracking Non-convex Extended Objects," *IEEE Trans. Aerosp. Electron. Syst.*, vol. 52, no. 6, pp. 2990-3007, 2016.

[9] M. Kumru, H. Köksal, and E. Özkan, "Variational Measurement Update for Extended Object Tracking Using Gaussian Processes," *IEEE Signal Process. Lett.*, vol. 28, pp. 538542, 2021.

[10] B. Tuncer, U. Orguner and E. Özkan, "Multi-Ellipsoidal Extended Target Tracking with Variational Bayes Inference," *IEEE Trans. Signal Process.*, vol. 70, pp. 3921-3934, 2022.

[11] B. Tuncer and E. Özkan, "Random Matrix Based Extended Target Tracking with Orientation: A New Model and Inference," *IEEE Trans. Signal Process.*, vol. 69, pp. 1910-1923, 2021.

[12] G. Battistelli, L. Chisci, G. Mugnai, A. Farina and A. Graziano, "Consensus-Based Linear and Nonlinear Filtering," *IEEE Trans. Autom. Control*, vol. 60, no. 5, pp. 1410-1415, 2015.

[13] W. Li, Y. Jia, D. Meng and J. Du, "Distributed Tracking of Extended Targets Using Random Matrices," in *Proc. 2015 54th IEEE Conf. on Decision and Control (CDC)*, Osaka, Japan, Feb. 2015, pp. 3044-3049.

[14] J. Hua and C. Li, "Distributed Variational Bayesian Algorithms for Extended Object Tracking," arXiv Preprint *arXiv: 1903.00182*, 2019.

[15] J. Liu and G. Guo, "Distributed Asynchronous Extended Target Tracking Using Random Matrix," *IEEE Sensors Journal*, vol. 20, no. 2, pp. 947-956, 2020.

[16] Y. Ren and W. Xia, "Distributed Extended Object Tracking Based on Diffusion Strategy," in *Proc. 28th European Signal Process. Conf. (EUSIPCO)*, Amsterdam, Netherlands, Jan. 2021, pp. 2338-2342.

[17] Z. Li, Y. Liang, L. Xu and S. Ma, "Distributed Extended Object Tracking Information Filter over Sensor Networks," *Int. J. Robust Nonlinear Control*, vol. 33, no. 2, pp. 1122-1149, 2023.

[18] Z. Li, H. Wang, S. Yan, H. Zou and M. Du, "Distributed Extended Object Tracking Filter Through Embedded ADMM Technique, in *Proc. 2022 IEEE Int. Conf. Multisensor Fusion and Integration for Intell. Syst. (MFI)*, Bedford, United Kingdom, Oct. 2022, pp. 1-6.

[19] H. Caesar et al., "nuScenes: A Multimodal Dataset for Autonomous Driving," in *Proc. 2020 IEEE/CVF Conf. Comput. Vis. Pattern Recognit.*, Seattle, WA, USA, June 2020, pp. 11618-11628.

$$
\begin{aligned}
\hat{\mathbf{J}}_{1k,x}^{(i-1)} &= \left.\frac{\partial \mathbf{S}_{1,k}}{\partial \boldsymbol{x}_k}\right|_{\hat{\boldsymbol{x}}_{k|k}^{(i-1)}} \\
&= \left.\begin{bmatrix} 0 & 0 & l_{k,1}(d_3 \sin\beta_k + d_1 \cos\beta_k) & l_{k,1}(d_2 \sin\beta_k + d_3 \cos\beta_k) & \frac{l_{k,1}(v_k^{\mathsf{x}} - v_k^{\mathsf{y}} \cot(\beta_k))}{\|\boldsymbol{\vartheta}_k\|} & \frac{l_{k,1}(v_k^{\mathsf{y}} - v_k^{\mathsf{x}} \tan(\beta_k))}{\|\boldsymbol{\vartheta}_k\|} \\ 0 & 0 & l_{k,2}(d_1 \sin\beta_k - d_3 \cos\beta_k) & l_{k,2}(d_3 \sin\beta_k - d_2 \cos\beta_k) & \frac{-l_{k,2}(v_k^{\mathsf{y}} + v_k^{\mathsf{x}} \cot(\beta_k))}{\|\boldsymbol{\vartheta}_k\|} & \frac{l_{k,2}(v_k^{\mathsf{x}} + v_k^{\mathsf{y}} \tan(\beta_k))}{\|\boldsymbol{\vartheta}_k\|} \end{bmatrix}\right|_{\hat{\boldsymbol{x}}_{k|k}^{(i-1)}},
\end{aligned} \tag{37}
$$

$$
\begin{aligned}
\hat{\mathbf{J}}_{2k,x}^{(i-1)} &= \left.\frac{\partial \mathbf{S}_{2,k}}{\partial \boldsymbol{x}_k}\right|_{\hat{\boldsymbol{x}}_{k|k}^{(i-1)}} \\
&= \left.\begin{bmatrix} 0 & 0 & l_{k,1}(d_3 \cos\beta_k - d_1 \sin\beta_k) & l_{k,1}(d_2 \cos\beta_k - d_3 \sin\beta_k) & \frac{l_{k,1}(v_k^{\mathsf{y}} + v_k^{\mathsf{x}} \cot(\beta_k))}{\|\boldsymbol{\vartheta}_k\|} & \frac{-l_{k,1}(v_k^{\mathsf{x}} + v_k^{\mathsf{y}} \tan(\beta_k))}{\|\boldsymbol{\vartheta}_k\|} \\ 0 & 0 & l_{k,2}(d_3 \sin\beta_k + d_1 \cos\beta_k) & l_{k,2}(d_2 \sin\beta_k + d_3 \cos\beta_k) & \frac{l_{k,2}(v_k^{\mathsf{x}} - v_k^{\mathsf{y}} \cot(\beta_k))}{\|\boldsymbol{\vartheta}_k\|} & \frac{l_{k,2}(v_k^{\mathsf{y}} - v_k^{\mathsf{x}} \tan(\beta_k))}{\|\boldsymbol{\vartheta}_k\|} \end{bmatrix}\right|_{\hat{\boldsymbol{x}}_{k|k}^{(i-1)}},
\end{aligned} \tag{38}
$$

$$
\hat{\mathbf{J}}_{1k,l}^{(i-1)} = \left.\frac{\partial \mathbf{S}_{1,k}}{\partial \boldsymbol{l}_k}\right|_{\hat{\boldsymbol{l}}_{k|k}^{(i-1)}} = \left.\begin{bmatrix} \frac{v_k^{\mathsf{x}} \cos\beta_k + v_k^{\mathsf{y}} \sin\beta_k}{\|\boldsymbol{\vartheta}_k\|} & 0 \\ 0 & \frac{v_k^{\mathsf{x}} \sin\beta_k - v_k^{\mathsf{y}} \cos\beta_k}{\|\boldsymbol{\vartheta}_k\|} \end{bmatrix}\right|_{\hat{\boldsymbol{l}}_{k|k}^{(i-1)}}, \tag{39}
$$

$$
\hat{\mathbf{J}}_{2k,l}^{(i-1)} = \left.\frac{\partial \mathbf{S}_{2,k}}{\partial \boldsymbol{l}_k}\right|_{\hat{\boldsymbol{l}}_{k|k}^{(i-1)}} = \left.\begin{bmatrix} \frac{v_k^{\mathsf{y}} \cos\beta_k - v_k^{\mathsf{x}} \sin\beta_k}{\|\boldsymbol{\vartheta}_k\|} & 0 \\ 0 & \frac{v_k^{\mathsf{y}} \sin\beta_k + v_k^{\mathsf{x}} \cos\beta_k}{\|\boldsymbol{\vartheta}_k\|} \end{bmatrix}\right|_{\hat{\boldsymbol{l}}_{k|k}^{(i-1)}}. \tag{40}
$$

---

[20] A. Scheel and K. Dietmayer, “Tracking Multiple Vehicles Using a Variational Radar Model,” *IEEE Trans. Intell. Transp. Syst.*, vol. 20, no. 10, pp. 37213736, 2018.

[21] Y. Xia, P. Wang, K. Berntorp, H. Mansour, P. Boufounos, and P. V. Orlik, “Extended Object Tracking Using Hierarchical Truncation Model with Partial-View Measurements,” in *Proc. 2020 IEEE 11th Sensor Array and Multichannel Signal Process. Workshop (SAM)*, Hangzhou, China, June 2020, pp. 1-5.

[22] K. Thormann, S. Yang and M. Baum, “Kalman Filter Based Extended Object Tracking with a Gaussian Mixture Spatial Distribution Model,” in *Proc. 2021 IEEE Intell. Veh. Symposium Workshops (IV Workshops)*, Nagoya, Japan, Jan. 2021, pp. 293-298.

[23] S. Liu, Y. Liang, L. Xu, T. Li, and X. Hao, “EM-based Extended Object Tracking Without a Priori Extension Evolution Model,” *Signal Process.*, vol. 188, pp. 108181, 2021.

[24] Z. Li, Y. Liang and L. Xu, “Distributed Extended Object Tracking Using Coupled Velocity Model from WLS Perspective,” *IEEE Trans. Signal Inf. Process. Netw.*, vol. 8, pp. 459-474, 2022.

[25] M. Li, J. Lan and X. R. Li, “Tracking of Elliptical Extended Object with Unknown but Fixed Lengths of Axes,” in *Proc. 2020 IEEE 23rd Int. Conf. Inf. Fusion*, Rustenburg, South Africa, Sept. 2020, pp. 1-8.

[26] N. Yokoyama, “Parameter Estimation of Aircraft Dynamics via Unscented Smoother with Expectation-Maximization Algorithm,” *J. Guid. Control Dynam.*, vol. 34, no. 2, pp. 426436, 2011.